Static-light hadrons on a dynamical anisotropic lattice

Justin Foley[*]**, Alan Ó Cais, Mike Peardon, Sinéad M. Ryan, Jon-Ivar Skullerud**
School of Mathematics, Trinity College, Dublin, Ireland
Email: `fly@maths.tcd.ie`

We present preliminary results for the static-light meson and baryon spectra for $N_f = 2$ QCD. The study is performed on an anisotropic lattice and uses a new all-to-all propagator method allowing us to determine particle masses to a high precision.

XXIIIrd International Symposium on Lattice Field Theory
25-30 July 2005
Trinity College, Dublin, Ireland

[*]Speaker.

1. Introduction

The simulation of hadrons containing one or more heavy quarks has been at the forefront of lattice QCD calculations for many years. Such hadrons can be problematic for lattice calculations because systematic errors which scale with the quark mass can make simulations with isotropic relativistic actions unreliable. The static limit, NRQCD and the Fermilab approach have all been used for simulations with *b* quarks as have simulations at lighter quarks which are then extrapolated to the bottom quark mass. Results from the static limit can also be combined with those of lighter quarks to make an interpolation to the *b* quark mass.

The static limit, where $m_Q \to \infty$, is the lowest-order term in a $1/m_Q$ expansion of the Heavy Quark Effective Theory (HQET) Lagrangian. In this limit the approximate heavy quark spin and flavour symmetries become exact. It is believed that calculations in this limit can be relevant to *b*-physics; however, historically the signal-to-noise ratio in static-light correlation functions has been particularly poor. All-to-all propagators have been used in previous static-light simulations since they lead to an increase in statistics by placing the source and sink operators at every spatial site on the lattice [1, 2]. More recently, in Ref [3] a modified static quark action has been shown to give improved discretisation errors and signal-to-noise ratios in correlation functions.

In this work, all-to-all propagators are used on anisotropic lattices for optimal determination of the particle energies. This algorithm has been described in detail in Ref [4].

A 3+1 anisotropic action is used with $N_f = 2$. The gauge action is a two-plaquette Symanzik-improved action which is described in Ref [5]. The quark action has been designed for large anisotropies. The usual Wilson term appears in the fine temporal direction and doublers are removed in the coarse spatial directions by a Hamber-Wu term. Further details can be found in Ref [6]. This action is written

$$S_q = \bar{\psi} \left(\gamma_0 \nabla_0 + \sum_i \mu_r \gamma_i \nabla_i \left(1 - \frac{1}{6} a_s^2 \Delta_i \right) - \frac{ra_t}{2} \Delta_0 + s a_s^3 \sum_i \Delta_i^2 + m_0 \right) \psi. \qquad (1.1)$$

where $\mu_r = (1 + \frac{1}{2} r a_t m_0)$, $r = 1$ is the usual coefficient of the Wilson term in the temporal direction and $s = \frac{1}{8}$ is the analogous coefficient in the spatial directions.

2. The static-light spectrum

The static-light spectrum of hadrons can be classified according to the angular momentum of the light degrees of freedom, J_l. For static-light mesons the *S*, *P* and *D* wave states have

$$J_l = \underbrace{\frac{1}{2}^-}_{\textbf{S}}, \underbrace{\frac{1}{2}^+, \frac{3}{2}^+}_{\textbf{P}}, \underbrace{\frac{3}{2}^-, \frac{5}{2}^-}_{\textbf{D}}. \qquad (2.1)$$

Interpolating operators are constructed for the light degrees of freedom which transform according to the irreducible representations of O_h. The relation between these irreducible representations and continuum quantum numbers can be determined by subduction. Table 1 lists the irreducible representations of the proper subgroup *O* as well as the angular momenta of the lower-lying corresponding continuum states. Note that, for example, to study the *D*-wave mesons requires operators

Lattice Irrep	Dimension	Continuum Irreps
A_1	1	$0, 4, \ldots$
A_2	1	$3, \ldots$
E	2	$2, 4, \ldots$
T_1	3	$1, 3, \ldots$
T_2	3	$2, 3, \ldots$
G_1	2	$\frac{1}{2}, \frac{7}{2}, \ldots$
G_2	2	$\frac{5}{2}, \frac{7}{2}, \ldots$
H	4	$\frac{3}{2}, \frac{5}{2}, \ldots$

Table 1: The irreducible representations of the lattice rotation group, *O* and their continuum analogues.

in the G_2 and H irreducible representations. To construct the operators needed in a study of S, P and D wave states single-link and planar-diagonal displacements were used.

3. Results

The preliminary results described here were obtained on dynamical lattices with $N_f = 2$ and stout-link smeared gauge configurations [7]. All-to-all propagators [4, 8] with two sets of time-diluted noise vectors were used to improve the resolution of signals and enable us to determine both mesons and baryons. This lowest level of dilution was sufficient to obtain good signals in our static-light simulation. Five levels of Jacobi smearing were applied to the light quark fields and the two-point static-light correlation function was subsequently optimised using variational techniques.

The simulation parameters for this study are given in Table 2. The ratio of scales $\xi = a_s/a_t$ is 6 and the intricacies of non-perturbatively tuning the gauge and fermion anisotropy, ξ, are discussed in Ref [9]. The results presented here are determined on a lattice extended in the temporal direction.

Volume	$8^3 \times 80$
Configurations	176 (mesons); 136 (baryons)
β	1.5
a_s	0.21fm
$a_t m_{\text{sea}}, a_t m_{\text{light}}$	-0.057
m_π/m_ρ	0.55

Table 2: Simulation parameters. The light and sea quark masses are close to the strange quark and their negative value in this table is an artefact of the Wilson additive quark mass renormalisation.

This is motivated by our initial studies of the static-light mesons on an $8^3 \times 48$ lattice. The quality of the data is now so good on these lattices that a very slowly falling signal was observed. This could not have been resolved with larger statistical errors. The comparison of data from the $8^3 \times 48$ and the $8^3 \times 80$ lattice is presented in Figure 1. The plot clearly shows that the longer lattice allows for a more reliable determination of the energy. The statistical errors are less than a percent in the region where a plateau is observed.
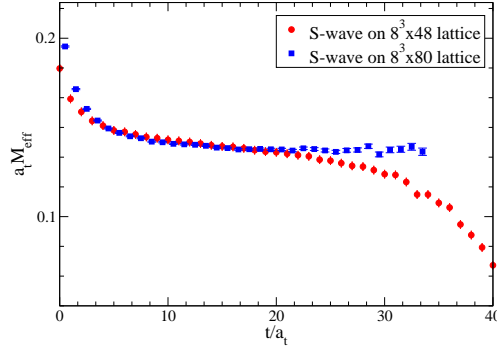
Figure 1: A comparison of the effective mass of a static-light meson on $8^3 \times 80$ and $8^3 \times 48$ lattices. The longer lattice allows a more reliable determination of the ground state.

3.1 Mesons

Figure 2 shows the effective masses of the static-light meson S, P and D waves. The states are labelled by their lattice irreducible representations and the corresponding continuum spin-states are listed in Table 1. The plot demonstrates that all-to-all propagators yield a dramatic improvement in signal quality and allow the resolution of excited states. In the static limit mass splittings can
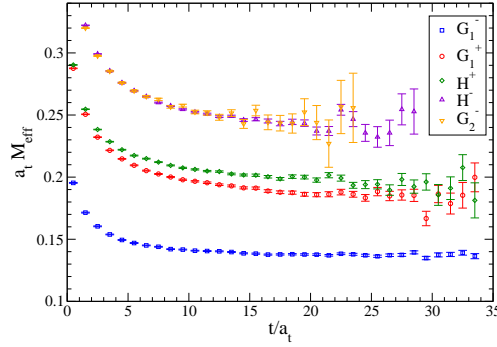

Figure 2: Effective masses of the orbitally-excited static-light meson. States are labelled as in Table 1 and by the parity of the meson.

be straightforwardly compared to their continuum values. In this study we find that these splittings can be determined very precisely. Figure 3 shows our preliminary results for the $P-S$ splitting and the splitting between the $\frac{3}{2}^+$ and $\frac{1}{2}^+$ P-wave states. We find that the $\Delta M(P-S) = 0.0481(8)$ and $\Delta M(P_{\frac{3}{2}^+} - P_{\frac{1}{2}^+}) = 0.0119(7)$. Figure 4 shows preliminary results for the $D-S$ splitting. The states are labelled by the irreducible representations of O (as in Table 1) and the parity of the meson. Within errors, no splitting is observed between the lowest-lying states in the G_2^- and H^- channels. This may indicate the inversion of the natural ordering of the D-wave multiplet predicted by some quark models, implying that the $\frac{3}{2}^-$ D-wave is in fact heavier than the $\frac{5}{2}^-$ D-wave. This has not been observed in other lattice studies. However, these are preliminary results and a conclusive statement can only be drawn when we have analysed the systematic errors including finite volume and discretisation effects. This is work in progress. The minimum timeslices used in Figures 3 and 4 is chosen by demanding that the effective masses of the particles involved have also reached
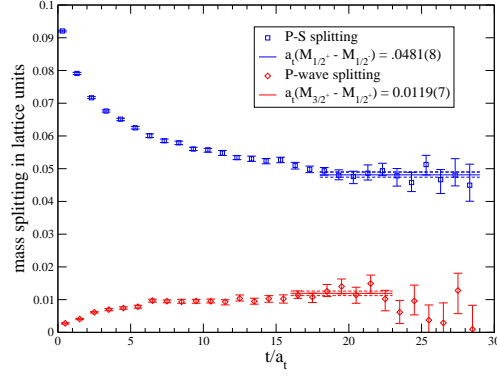
Figure 3: The mass-splitting between S and P wave states (blue points) and between the $\frac{3}{2}^{+}$ and $\frac{1}{2}^{+}$ P wave states (red points). The solid lines are best fits to the splittings (not the difference of fits to effective masses).
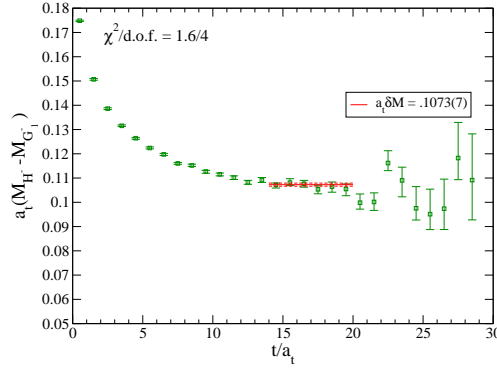

Figure 4: The mass-splitting between the D and S waves, labeled H^{-} and G_{1}^{-} respectively.

a plateau at this time.

3.2 Baryons

Using all-to-all propagators we have constructed local operators for the isoscalar (Λ_b) $\frac{1}{2}^{+}$ and the isovector (Σ_b) $\frac{3}{2}^{+}$ baryons. The projectors, $\frac{1}{2}(1+\gamma_0)$ and $\frac{1}{2}(1-\gamma_0)$, applied to the light quark fields, as well as time-reversal symmetry, were used to improve signals in fits to the effective masses. Figure 5 shows the effective masses of the Λ_b and Σ_b. The effective mass of the B meson is included for reference. The mass splittings are $a_t\Delta = 0.68(2)$ and $a_t\Delta = 0.078(14)$ for the Λ_b and Σ_b resectively.

4. Conclusions and outlook

In this paper we have presented preliminary results for the masses and mass-splittings of static-light mesons and baryons, with $N_f = 2$. Using all-to-all propagators and anisotropic lattices, excellent signals for the B-meson and its radial excitations: P and D waves are found. Mesons are determined from 176 configurations while 136 configurations are used to study baryons. Even for this preliminary dataset, splitting between P and S waves, between P waves and between D and S waves can be determined at the percent level. Our results also suggest an inversion in the natural
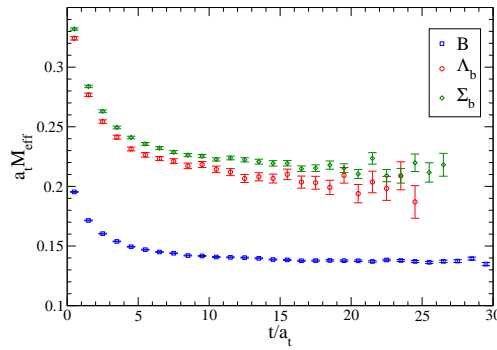
Figure 5: The effective masses of the isoscalar (Λ_b) $\frac{1}{2}^+$ and the isovector (Σ_b) $\frac{3}{2}^+$ baryons.

ordering in the *D*-wave multiplet. This warrants further study and is work in progress. The masses of the Λ_b and Σ_b baryons and their splittings are also determined. These results are very encouraging and we plan to extend this study to larger volumes with correctly renormalised parameters, ξ_q and ξ_g.

Acknowledgments

References

[1] **UKQCD** Collaboration, C. Michael and J. Peisa, *Maximal variance reduction for stochastic propagators with applications to the static quark spectrum*, *Phys. Rev.* **D58** (1998) 034506 [hep-lat/9802015].

[2] **UKQCD** Collaboration, A. M. Green, J. Koponen, C. McNeile, C. Michael and G. Thompson, *Excited B mesons from the lattice*, *Phys. Rev.* **D69** (2004) 094505 [hep-lat/0312007].

[3] **ALPHA** Collaboration, M. Della Morte *et. al.*, *Lattice HQET with exponentially improved statistical precision*, *Phys. Lett.* **B581** (2004) 93–98 [hep-lat/0307021].

[4] J. Foley *et. al.*, *Practical all-to-all propagators for lattice QCD*, hep-lat/0505023.

[5] C. Morningstar and M. J. Peardon, *The glueball spectrum from novel improved actions*, *Nucl. Phys. Proc. Suppl.* **83** (2000) 887–889 [hep-lat/9911003].

[6] **TrinLat** Collaboration, J. Foley, A. Ó Cais, M. Peardon and S. M. Ryan, *A non-perturbative study of the action parameters for anisotropic-lattice quarks*, hep-lat/0405030.

[7] C. Morningstar and M. J. Peardon, *Analytic smearing of SU(3) link variables in lattice QCD*, *Phys. Rev.* **D69** (2004) 054501 [hep-lat/0311018].

[8] **TrinLat** Collaboration, A. Ó Cais, K. J. Juge, M. J. Peardon, S. M. Ryan and J.-I. Skullerud, *Improving algorithms to compute all elements of the lattice quark propagator*, hep-lat/0409069.

[9] R. Morrin, M. Peardon and S. M. Ryan, *Tuning anisotropies for dynamical gauge configurations*, PoS **(LAT2005)** 236 [hep-lat/0510016].